

The influence of Cr on structure and thermal expansion of copper matrix composites reinforced with unidirectionally aligned continuous high modulus C fibres

N. Beronská*, K. Iždinský, P. Štefánik, F. Simančík, M. Zemánková, T. Dvorák

Institute of Materials and Machine Mechanics, Slovak Academy of Sciences, Račianska 75, 831 02 Bratislava, Slovak Republic

Received 1 April 2009, received in revised form 11 May 2009, accepted 12 May 2009

Abstract

The influence of Cr on structure and thermal expansion of copper matrix composites reinforced with unidirectionally aligned continuous high modulus K1100 carbon fibres was studied. It appears that the addition of 1 wt.% of Cr has dramatically improved the wetting of K1100 fibres with the matrix alloy CuCr1, facilitating thus the composite preparation via gas pressure infiltration. Due to the chemical reaction with K1100 fibres a reactive interfacial bonding has been formed. The lack of wetting resulted in larger voids and weak interfacial bonding in Cu-K1100 fibres.

The results of thermal expansion measurements confirmed large anisotropy of properties as well as very good structural stability of both composites exhibiting no signs of possible disintegration. This however will have to be further confirmed by increasing the number of thermal cycles. The effect of Cr on the thermal expansion of composites under investigation was found less apparent as in short fibre or particulate reinforced composites.

Key words: metal matrix composite, high modulus K1100 carbon fibres, copper matrix-carbon fibres interface, thermal expansion

1. Introduction

Two main tasks dominate the modern heat sink design in electronic applications, particularly in laser diodes, central processing units and power electronic devices. These are faster heat removal and minimization of thermal stresses. Faster heat removal can be achieved by higher thermal conductivity (TC) and thermal stresses can be reduced by modifying the coefficient of thermal expansion (CTE) of heat sink.

It appears that the first and second-generation substrate materials e.g. Cu, Cu-Mo, Cu-W, and Al-SiC are no longer sufficient to fulfil the requirements [1, 2] and new heat sink materials with improved properties are to be explored. The substantial contribution is expected from composite materials where metal matrix is reinforced with high TC and low CTE phases. Currently the preferential reinforcing phase is carbon with many of its allotropic modifications – dia-

mond, flakes, fibres, nanotubes, etc. with TC as high as $3300 \text{ W m}^{-1} \text{ K}^{-1}$ (synthetic diamond) and CTE as low as $-1.5 \times 10^{-6} \text{ K}^{-1}$ (high modulus carbon fibres). However, their actual potential in terms of feasibility, interfacial bonding, heterogeneity of properties, machineability, costs, etc. still needs to be further explored.

Best conducting matrices are silver ($430 \text{ W m}^{-1} \text{ K}^{-1}$) and copper ($400 \text{ W m}^{-1} \text{ K}^{-1}$), however the latter is more perspective for large-scale production because of cost reasons. Anyway, combining of C phases with Cu matrix faces several difficulties. These include no wetting and the lack of chemical activity in the Cu-C binary system resulting in poor bonding at the interface, with implications towards TC and CTE. Therefore active elements need to be added to copper matrix to improve the interface.

This was demonstrated several times. The evaluation of the TC and the CTE as a function of the

*Corresponding author: tel.: + 421 2 49 268 228; fax: + 421 2 44 253 301; e-mail address: ummsnfra@savba.sk

Table 1. Properties of K1100 carbon fibres

Tensile strength (GPa)	3.10
Tensile modulus (GPa)	965
Density (kg m^{-3})	2200
Filament diameter (μm)	10
Carbon assay (%)	99+
Surface area ($\text{m}^2 \text{kg}^{-1}$)	400
Electrical resistivity ($\mu\Omega \text{m}$)	1.1–1.3
Thermal conductivity in longitudinal direction ($\text{W m}^{-1} \text{K}^{-1}$)	900–1000
Thermal conductivity in transversal direction ($\text{W m}^{-1} \text{K}^{-1}$)	2.4
Longitudinal CTE at 21 °C (K^{-1})	-1.5×10^{-6}
Transversal CTE at 21 °C (K^{-1})	12.0×10^{-6}

alloying content of Cr and B in the copper matrix in Cu-X/diamond composites prepared by gas pressure assisted liquid metal infiltration is presented in [3]. In both systems with diamond content ~ 60 vol.% a transition from weak matrix/diamond bonding to strong bonding is observed, the latter leading concomitantly to high TC ($> 600 \text{ W m}^{-1} \text{K}^{-1}$) and low CTE ($< 10 \times 10^{-6} \text{ K}^{-1}$). Similarly, in copper/diamond composites prepared by powder metallurgy the TC increased from $\sim 200 \text{ W m}^{-1} \text{K}^{-1}$ for pure copper matrix to $\sim 640 \text{ W m}^{-1} \text{K}^{-1}$ for copper matrix alloyed with 0.8 wt.% of Cr [4, 5].

The effect of interfacial bonding on the TC behaviour was studied on unidirectional SiC fibre-reinforced Cu-matrix composites [6]. Composites with about 25 vol.% of SiC fibres with or without Ti6Al4V sputtered coatings as adhesion promoters were prepared by hot pressing. The thermal expansion measurements revealed that the strong interfacial bonding (via Ti6Al4V) could significantly reduce the longitudinal CTE of the composite close to theoretical values predicted by Scharpery's model. The weak interface (without Ti6Al4V) is not just unable to effectively reduce the CTE, but is also unable to control the dimensional stability after some thermal cycles.

Wang et al. [7] studied the effect of interfacial bonding strength on the thermal expansion of Cu/C composites prepared by hot pressing. They found that all the composites (with or without Fe or Ni as interfacial adhesion promoters) had positive residual strains after a full thermal cycle, and interfacial bonding strength had significant influence on the residual strain: namely the higher the interfacial bonding strength, the smaller the residual strain. On the other hand, other studies confirm a permanent dimensional reduction of some composites when the bonding strength between reinforcement and matrix is excellent [8, 9].

High modulus and high TC carbon fibres represent a specific variant of advanced continuous C phases. When combined with Cu matrix, composites with very high TC and low CTE can be reasonably expected. The unidirectional alignment of continuous fibres

provides specific properties to composite where the role of interfacial bonding strength is modified particularly when compared to short fibre or particulate reinforced composites. The effect of weak and strong interface on thermal expansion of copper based matrix – high modulus and high TC carbon fibre reinforced composites is examined in this work.

2. Experimental material and procedure

High modulus pitch based Thornel K1100 carbon fibres with 2000 filaments in one tow have been used as uniaxially aligned reinforcement in two copper based matrices. These included binary CuCr1 alloy with 1 wt.% of Cr and pure copper with the purity of 99.99 %. The properties of C fibres are presented in Table 1. Gas pressure infiltration was employed as the preferred consolidation technique.

As-received fibres were unidirectionally aligned and slightly pressed into a Mo mould forming thus a fibrous preform. These rod-like preforms with the dimensions $13 \times 13 \times 60 \text{ mm}^3$ had been inserted into a high pressure autoclave and preheated in a vacuum $\sim 100 \text{ Pa}$. Once the infiltration temperature of $1200 \text{ }^\circ\text{C}$ had been reached, the system was allowed to thermally equilibrate for roughly 30 min. Fibre preforms were subsequently immersed into a graphite crucible with a molten matrix metal. The crucible walls were preliminarily coated with boron nitride in order to avoid the reaction of CuCr1 alloy with graphite. Nitrogen gas pressure was applied up to 6.0 MPa within 5 minutes. The infiltration with CuCr1 alloy was relatively easy due to improved wetting. Infiltration with pure Cu was quite tricky and a proper way of metal penetration had to be optimized.

Structural observations on as-received samples were performed with light microscopy (LM – OLYMPUS GX51) and secondary electron microscopy (SEM – JEOL JSM 5310). Chemical compositions were analysed using energy dispersive X-ray spectroscopy (EDXS – KEVEX DELTA IV).

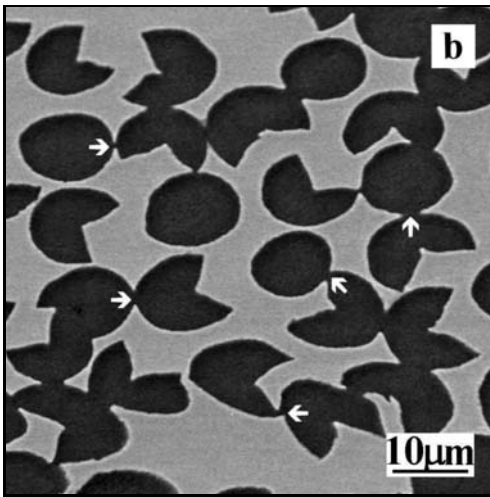
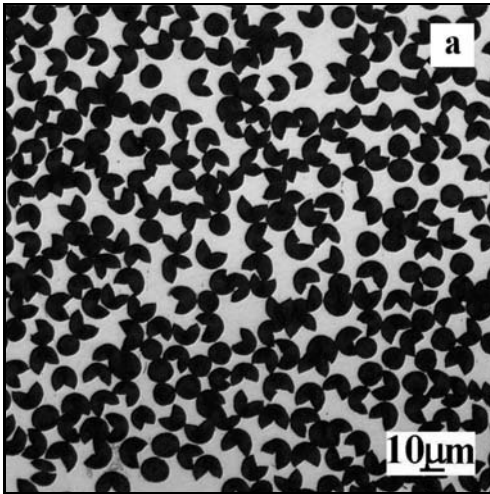


Fig. 1. Cross sectional view of CuCr1-K1100 composite: a) light micrograph and b) secondary electron micrograph.

Composite samples with the dimensions $4 \times 4 \times 10 \text{ mm}^3$ were used for linear thermal expansion measurements in both longitudinal (L) and transversal (T) directions. Designation L and T corresponds to fibre alignment direction with respect to longitudinal sample axes. Samples were subjected to three consequent heating and cooling cycles at the heating/cooling rate of 3 K min^{-1} in an argon atmosphere using LINSEIS L75VS 1600C dilatometer. Samples were cycled in the temperature range 30°C to 600°C . Each thermal cycle started with the sample preheating at 30°C for 30 minutes, followed by heating and subsequent cooling back to the room temperature. One-hour rest time had been included before the next cycle started.

Instantaneous CTE values were calculated from the strain-temperature curves as a function of temperature using LINSEIS TAWIN software. All CTEs were calculated in the temperature range 50°C to 550°C in order to eliminate the effect of non-steady state tran-

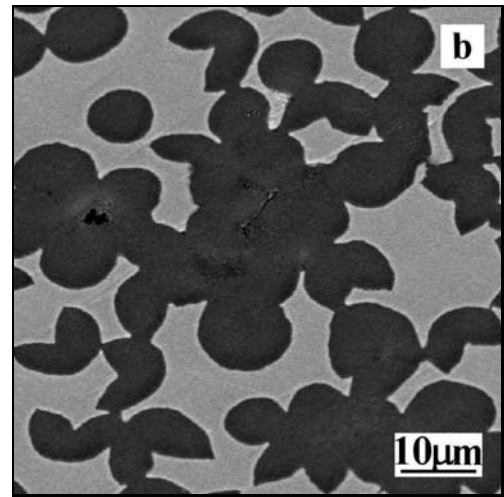
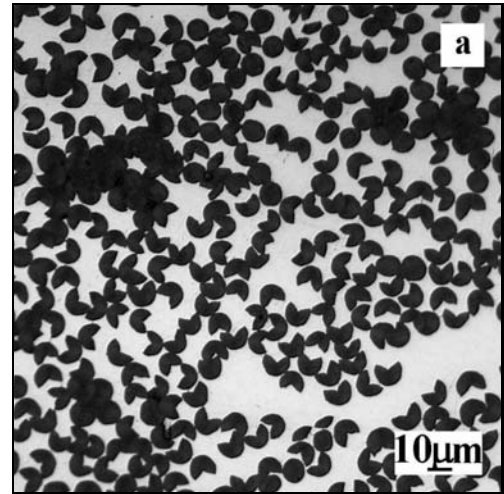


Fig. 2. Cross sectional view of Cu-K1100 composite: a) light micrograph and b) secondary electron micrograph.

sient stages occurring at the beginning and at the end of heating and cooling periods.

3. Results

3.1. Structural studies

Structure of the CuCr1-K1100 composite as observed by light microscopy is presented in Fig. 1a. As can be seen, relatively homogeneous distribution of C fibres in the sample was achieved. No large voids or poor infiltrated samples were observed. Almost each fibre is surrounded by the matrix metal indicating satisfactory wetting in the system. The average fibre volume content as determined via image analysis in 5 different locations is 54.76 %. The results obtained by light microscopy observations were further confirmed by scanning electron microscopy. Secondary electron micrograph of typical microstructure is presented in

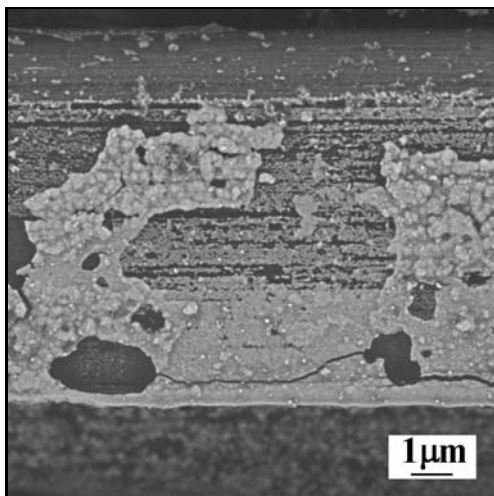


Fig. 3. Fibre surface with discontinuous chromium carbide in CuCr1-K1100 composite (secondary electron micrograph).

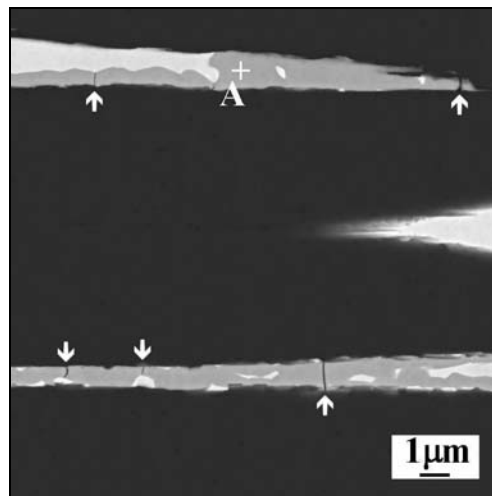


Fig. 5. Chromium carbide (grey) in inter-fibre location in longitudinal section of CuCr1-K1100 composite (secondary electron micrograph).

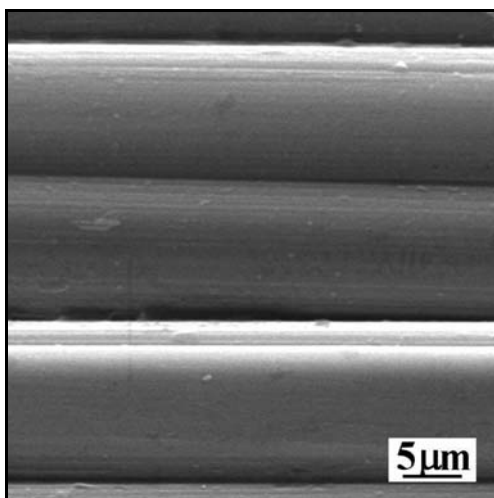


Fig. 4. Fibre surface in Cu-K1100 composite (secondary electron micrograph).

Fig. 1b. It can be seen that small voids are localized exclusively in points of contact of adjacent C fibres. Some are pointed out with white arrows.

Structure of the Cu-K1100 composite is presented in Fig. 2. As evident, the infiltration was not as good as in previous system. The average fibre volume content as determined via image analysis in 5 different locations is 53.69 %. However, fibres tended to merge into clusters where the molten metal did not entirely penetrate. Fibre clusters in Cu-K1100 composite are presented in Fig. 2b.

Fibre-matrix reaction was observed on fibre surfaces in the structure of deeply etched CuCr1-K1100 composite as shown in Fig. 3. This was quite different

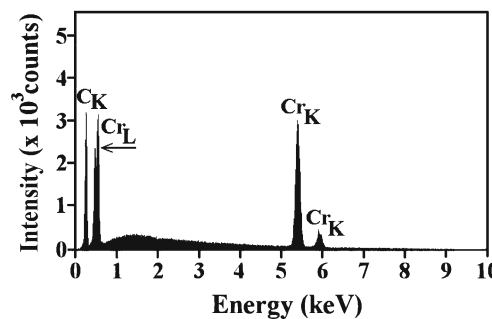


Fig. 6. EDX spectrum acquired from point A in Fig. 5.

from smooth fibres in Cu-K1100 composite presented in Fig. 4.

Reaction phase in CuCr1-K1100 composite is presented in Fig. 5. It appears grey and is located in inter-fibre locations. EDX analysis in Fig. 6 confirmed C and Cr in the reaction product having indicated it as chromium carbide. However, the accuracy of measurements did not allow distinguishing between particular types of Cr_xC_y carbides. Anyway, the carbide is brittle as confirm numerous cracks oriented in perpendicular direction with respect to fibre alignment. The cracks propagate exclusively in carbide, being stopped at carbide-matrix and carbide-fibre interfaces.

The frequency of appearance of carbides was not constant along the fibre length. They were formed more frequently on fibre surfaces oriented towards the larger metal volumes inside the sample. The reaction was also more often observed closer to sample surface that had been in contact with the surrounding matrix metal in crucible. Chromium carbides appeared rather continuous near the surface and more localized

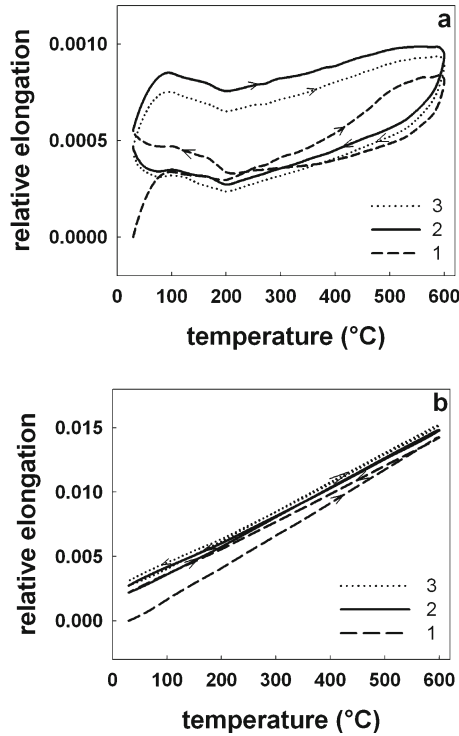


Fig. 7. Temperature dependences of relative elongation of CuCr1-K1100 composite subjected to three consecutive thermal cycles in a) *L* and b) *T* directions.

to small islands inside the sample. No Cr has been found in the matrix of as-prepared CuCr1-K1100 composite indicating that all Cr had been consumed in the fibre-matrix reaction.

3.2. Thermal expansion

The temperature dependences of relative elongation and CTE of CuCr1-K1100 composite are presented in Figs. 7 and 8. Large differences in relative elongations were recorded in *L* and *T* directions. At the end of the first thermal cycle a permanent relative elongation was recorded in *L* direction. The second and third cycles were nearly identical however with small permanent contractions. Permanent relative elongations corresponding to individual cycles are summarized in Table 2. All three cycles exhibit hysteresis

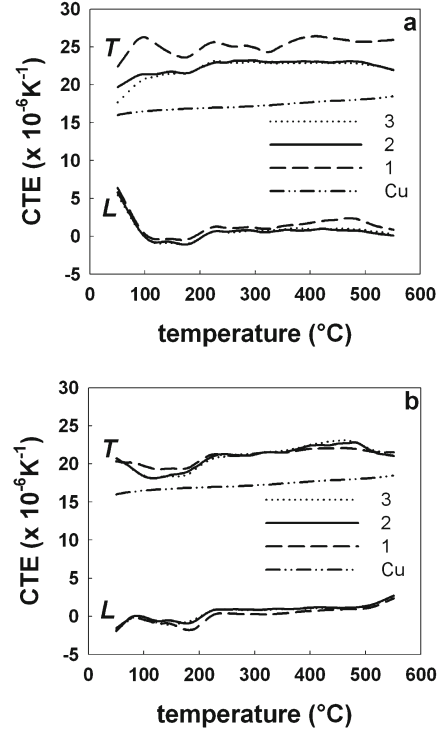


Fig. 8. Temperature dependences of CTE of Cu reference and CuCr1-K1100 composite subjected to three consecutive thermal cycles during a) heating and b) cooling periods.

– i.e. the heating and cooling values do not coincide.

Considerably larger permanent strains were recorded in *T* direction. The largest relative elongation appeared at the end of the first cycle. Second and third thermal cycles exhibited decreasing permanent elongations as shown in Table 2.

CTEs in Fig. 8 further confirm the anisotropy of the composite. They point out the different character of the first thermal cycle however the subsequent two cycles are nearly identical for both heating and cooling periods in *L* and *T* directions. The temperature dependences of CTE in the second and third cycles exhibit certain linearity in the temperature range 220 to 500 °C. The mean coefficients of thermal expansion in this temperature range are presented in Table 3. Comparison of obtained CTEs shows that the expansion

Table 2. Net permanent relative elongations as acquired per individual thermal cycle

Cycle No.	CuCr1-K1100		Cu-K1100	
	<i>L</i>	<i>T</i>	<i>L</i>	<i>T</i>
1	5.5×10^{-4}	21.8×10^{-4}	-4.5×10^{-4}	2.1×10^{-4}
2	-0.8×10^{-4}	5.4×10^{-4}	-0.2×10^{-4}	2.9×10^{-4}
3	-0.4×10^{-4}	3.8×10^{-4}	-0.4×10^{-4}	3.8×10^{-4}

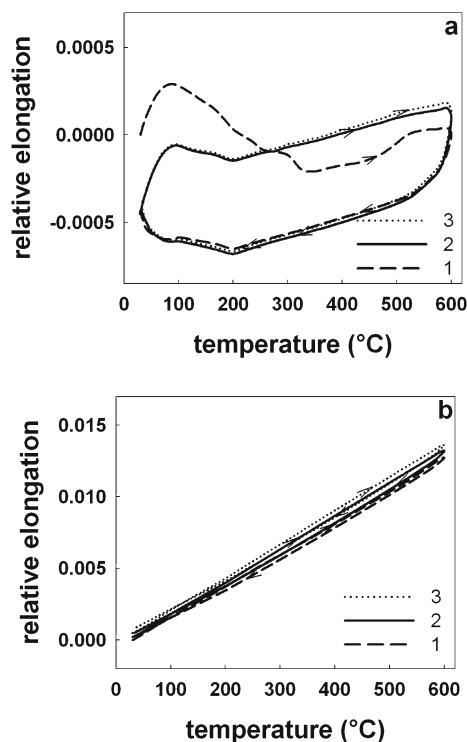


Fig. 9. Temperature dependences of relative elongation of Cu-K1100 composite subjected to three consecutive thermal cycles in a) L and b) T directions.

of composite in L direction is substantially lower than that of reference Cu demonstrating thus the thermal expansion reduction due to fibres. Complementary to this result, the expansion of composite in T direction is higher than that of reference Cu.

The temperature dependences of relative elongation and CTE of Cu-K1100 composite are presented in Fig. 9. Permanent relative contractions were recorded in L direction at the end of all three thermal cycles. The first thermal cycle exhibited the highest contraction, the second and third cycles were as in previous composite nearly identical. Cu-K1100 composite also exhibited hysteresis in all three cycles.

Permanent elongations were recorded at the end of all three cycles in T direction. As shown in Table 2, they were in a close range with the smallest elongation recorded at the end of the first thermal cycle.

CTEs in Fig. 10 further also confirm the different character of the first thermal cycle. This can be particularly seen in heating periods of both L and T directions. The second and third cycles are almost identical. The mean coefficients of thermal expansion in the temperature range 220°C to 500°C are summarized in Table 3. Comparison of obtained CTEs in Fig. 10 shows that the expansion of Cu-K1100 composite in L direction is substantially lower and in T direction higher than that of reference Cu.

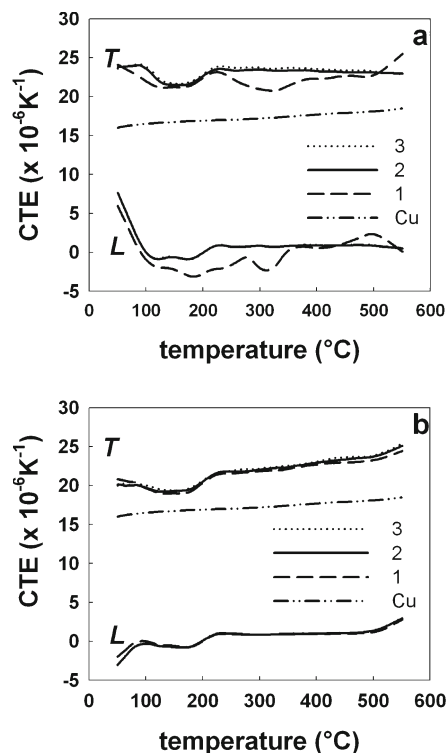


Fig. 10. Temperature dependences of CTE of Cu reference and Cu-K1100 composite subjected to three consecutive thermal cycles during a) heating and b) cooling periods.

Table 3. Average values of the coefficient of linear thermal expansion in the temperature range 220°C to 500°C

	CuCr1-K1100		Cu-K1100	
	heating	cooling	heating	cooling
CTE_L ($10^{-6} K^{-1}$)	0.8	1.0	0.8	1.0
CTE_T ($10^{-6} K^{-1}$)	23.0	21.9	23.5	22.7

4. Discussion

4.1. Structural studies

Cu-C composite materials can be prepared via solid-state diffusion bonding as demonstrated in [10]. This preparation route had required Cu coated C fibres that were subsequently consolidated into bulk composite by vacuum hot pressing at 700°C. The galvanic coating of fibres had been performed in a coating line, where the tows had to pass a complicated path including small bend radii on different rollers [11]. It was not too difficult for Torayca T300 high strength C fibres. However, high modulus K1100 fibres appeared to be too brittle to survive this procedure. Therefore the solid state compacting was not possible for Cu-K1100 composites.

Problems associated with continuous fibre reinforced composites prepared by melt infiltration include: 1. failure of the molten metal to penetrate narrow gaps between adjacent fibres; 2. intermetallic or reaction phase formation at fibre-matrix interfaces and 3. inhomogeneous distribution of fibres in composite [12]. The infiltration with CuCr1 alloy was relatively easy due to improved wetting caused by the addition of active metal. The most problematic sites were fibre contact locations where the interfacial and meniscus forces inhibit full melt penetration. Driving the liquid metal into these spaces between the reinforcing fibres is a complex process, dependent on several physical phenomena, which often make the application of pressure on the metal matrix a necessity [13].

Here the wetting mechanism plays an important role. This has already been extensively studied by Mortimer and Nicholas by sessile drop tests [14, 15]. They reported that small additions of Cr reduced the non-wetting contact angles formed by Cu on graphite from approximately 140 deg to 45–50 deg for Cu – 1 at.% Cr alloy. The reaction product at the interface was continuous and quantitatively determined to be Cr_3C_2 . Nogi et al. [16] have reported that graphite is wet by Cu-Cr alloys when Cr content is high enough to create a continuous layer at the interface. The thermodynamics of chromium carbide formation on graphite substrate is presented in [17]. The comparison of free energy of formation for each potentially stable carbide phase at 1130°C indicates that the most stable phase is Cr_3C_2 ($\Delta G = -4594$ cal/g·atom). The free energy of formation $\Delta G = -4065$ cal/g·atom corresponds to Cr_7C_3 and $\Delta G = -2741$ cal/g·atom to Cr_{23}C_6 formation. The thermodynamic analysis further indicates that Cr content in liquid Cu at 1130°C would have to be reduced to below 0.078 at.% before the formation of Cr_3C_2 would not be favourable [17].

Transferred sessile drop experiments conducted with Cu-Cr alloys on vitreous carbon substrates [18] showed, that the wetting was improved by drop-substrate chemical interaction, which led to the formation of a continuous wettable Cr_7C_3 carbide layer with the thickness 1 to 5 μm . As a consequence of interaction, the final contact angle decreases from 137° for pure Cu to about 40° for Cu alloyed with Cr.

The reality of gas pressure infiltration is far different from equilibrium sessile drop experiments. Moreover high modulus carbon fibres represent a specific carbon modification that makes the analysis of interfacial reactions even more difficult. Because of large surface area-to-volume ratio in realistic C-Cu composite, the extent of reaction layer thickness should be limited to, on average, a few nanometers by the Cr content in the Cu alloy. As presented in [17] for a fibre volume fraction of 50 % and 10 μm diameter of C fibres the surface area/volume is 200 mm^2/mm^3 . For a Cu-1.22 at.%Cr alloy matrix there is only enough Cr

available to form a Cr_3C_2 reaction layer 36 nm thick around the C fibres.

Generally, the presence of chromium carbide as a fibre-matrix reaction product was confirmed in this work. However, due to the accuracy of EDX analysis it was not possible to distinguish definitely between particular carbide phases. The analysis of published results confirms that both Cr_3C_2 and Cr_7C_3 were identified by X-ray diffraction methods in Cu-C composites.

More important, however, is the carbide morphology in the obtained samples. It appeared that continuous carbide layers could have been found in the surface locations of the sample. With increasing distance from the face or flank side of the sample, the carbide layers were less continuous and in the middle of the sample they appeared only rarely. This indicates that the temperature-time profile of the infiltration did not allow the establishment of equilibrium conditions for fibre-matrix reaction in the whole sample. Fibres close to the surface locations of the sample had been in a close contact with the fresh alloy from the crucible what resulted in an extensive reaction with Cr. On the other hand the fibres from the sample inside had been only in contact with relatively small volume of matrix alloy. Here Cr seems to be consumed relatively quickly and the short time of contact with molten metal did not allow re-establishing of the original Cr concentration.

Structural studies revealed cracks in chromium carbides. These seemed to be stopped at the carbide-fibre interface. This has most probably to do with the low length of the crack related to the low carbide thickness as well as with the internal fibre structure.

Carbon fibres are composed of 99.9 % pure carbon, most of each is arranged into a graphite crystallite. These crystallites tend to organize into layers preferentially oriented along the fibre longitudinal axis and the mechanical properties mostly reflect this structure. The high strength of graphite in the plane of atom lattice is stipulated by the non-polar nature of carbon atoms' interaction, whereas the low strength of graphite in case of tension in the perpendicular direction is the consequence of a very weak van der Waals type bond between the neighbouring layers. This may predominantly have a serious consequence to any load transfer at the fibre matrix interface. Particularly, even if the interfacial bonding is strong, the loading from the matrix can hardly be transferred to the fibre, as the shear strength of the neighbouring graphite layers is weak. Consequently if the crack propagates through the carbide to the fibre surface, it must be stopped there, while it is more favourable to propagate along the poorly bonded graphite planes.

Infiltration of C fibres with pure copper is due to poor wetting not trivial and a proper sequence of operational steps needs to be followed. Generally, C fibres tend to be pressed together forming closed

empty spaces where the penetration of molten metal is difficult. Here some separator particles, e.g. TiN as used in [19] can be helpful.

As shown in this work, molten copper can infiltrate the C fibrous preform also without the assistance of any third phase. The unidirectional alignment of continuous long fibres forms free channels in the inter-fibrous locations that enhance the molten metal penetration. However, the metal needs to enter the preform predominantly from the front (face) side. When it comes from the flank side it presses on fibres bringing them together in different mould locations and the fibre distribution is not homogeneous. The frequency of appearance of non-infiltrated locations increases in this case.

If there is enough space for the molten metal to penetrate into the preform it can fill the empty spaces. The external gas pressure can keep it there until solidification. Finally the matrix metal remains trapped in the inter-fibrous locations even without any interfacial reaction.

In any case the process of C fibre infiltration by pure Cu runs quite at the edge of stability. Although the molten metal is by the assistance of pressurized gas forced to penetrate into fibrous preform, it is at the same time rejected by fibre surfaces due to high wetting angle. The actual conditions determining the degree of penetration may locally vary to a large extent resulting in more or less successful infiltration. The stability of the process can hardly be maintained with larger samples, samples with more complicated shapes or with other than unidirectional fibre alignment.

4.2. Thermal expansion

The results of thermal expansion measurements confirmed large anisotropy of properties as well as very good structural stability of both composites exhibiting no signs of possible disintegration.

Comparison of the thermal expansion data reveals some distinctive characteristics including: different course of the temperature dependences of the relative elongation in the first thermal cycle for CuCr1-K1100 and Cu-K1100 composites, very similar relative elongations for both composites in the second and third cycles and finally two distinct knees appearing nearly at the same temperature of both composites in heating and cooling branches of relative elongations.

As shown in Figs. 7a and 9a, at the end of the first thermal cycle relative elongation was recorded for CuCr1-K1100 composite whereas relative contraction appeared for Cu-K1100 composite. As generally accepted, the residual strain in the first cycle strongly depends on the thermal and mechanical history of the material and it may have various origins, mechanical, thermal, or both. It may be removed by heating which

is associated with the permanent change of the specimen length. Rudajevová et al. [20] showed that the permanent reduction in the specimen length was observed in composite pre-deformed in tension, whereas permanent elongation was recorded in composite pre-deformed in compression. Positive residual strain recorded in the *L* direction of CuCr1-K1100 composite indicates that the as-received composite was in residual compression and the as-received Cu-K1100 composite exhibited negative residual strain in residual tension.

The residual thermal stresses occur in composite due to different thermal and mechanical properties of fibres and matrix. There are no thermal stresses within the composite at the matrix melting point. As the composite cools, the metal matrix contracts to a significantly larger extent than the fibre reinforcement. The thermal stresses are temperature dependent and they influence the dilatational characteristics of the composites [21].

The different residual stresses in as-received composites may be due to the chromium carbide at the interface in CuCr1-K1100 composite. The CTE of e.g. Cr₃C₂ is $10.3 \times 10^{-6} \text{ K}^{-1}$ [22] what is between that of Cu and K1100 fibres. This contributes to smaller stress generation through thermal expansion mismatch during thermal cycles. The significant contraction of Cu-K1100 composite in the course of heating in the first thermal cycle can be further related to the presence of pores and voids. If the interfacial bonding is weak, the matrix can easily expand into empty spaces decreasing thus the expansion significantly. The strong influence of voids on the thermal expansion of metal matrix composites was numerically and experimentally confirmed in [23].

However, residual strains appearing as a consequence of manufacturing process are mostly released during the first heating as revealed in related papers [6, 24–26]. This was confirmed also in this work.

Second and third cycles are nearly identical for both composites exhibiting no or very little permanent strain as presented in Fig. 11a. However, they exhibit two distinct knees on the temperature dependence of relative elongation. Relative elongations do rapidly increase in the temperature range 30 °C to 100 °C (first knee), then decrease in the range 100 °C to 200 °C (second knee) and finally monotonously increase up to 600 °C. Here, in the temperature range from 500 °C to 600 °C, a typical non-steady state transient stage occurs [27]. This is to be related to conversion of heating to cooling mode.

In the course of cooling, monotonous relative elongation decrease took place in the temperature range 600 °C down to 200 °C, followed by slight increase between 200 °C and 100 °C and a rapid increase between 100 °C and 30 °C.

This behaviour can be qualitatively explained tak-

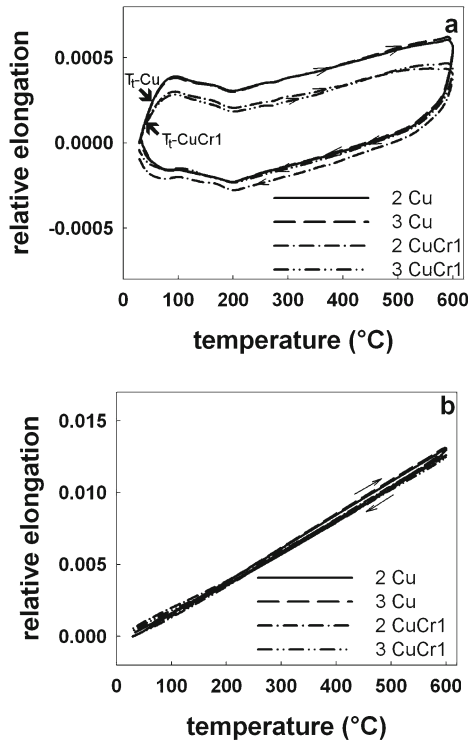


Fig. 11. Temperature dependence of relative elongations of CuCr1-K1100 and Cu-K1100 composites during second and third cycle in a) L and b) T directions.

ing into account the shear stress of the matrix and thermal expansion of fibres. Due to differences in CTE of matrix and fibres, matrix is in residual tension and fibres in residual compression after manufacturing cooling (as-received condition). As the CTE of matrix is $16.5 \times 10^{-6} \text{ K}^{-1}$ and that of fibres even negative $-1.5 \times 10^{-6} \text{ K}^{-1}$, the matrix residual tension is relatively quickly relieved during heating. Compressive stress in the matrix builds up with progressive heating. As soon as the compression yield stress is reached the operation of creep mechanism begins stress relief. The first knee is coincidental with the start of this stress relief leading to the decrease of relative elongation as analysed by Dutta [28]. In the case of strong interface this tendency would proceed up to the highest temperature. However, if the interfacial bonding strength becomes lower than the matrix shear strength, compressive stresses induced in the matrix are decreased relieving thus matrix for expansion. The second knee is likely to be associated with the decrease of the composite interfacial bonding strength.

Actually there is no reaction type of interfacial bonding in the Cu-K1100 composite. However, there is some mechanical bonding due to matrix shrinkage around fibres in the course of cooling. This bonding is released at heating as the matrix expands more than fibres with the positive value of CTE in transversal direction $\sim 12 \times 10^{-6} \text{ K}^{-1}$. This type of bonding can

be expected also in CuCr1-K1100 composite, as the interfacial reaction zone is not continuous. This might be the reason for similarity of both dependences shown in Fig. 11a.

Comparison of relative elongations further reveals that transition temperature T_t , i.e. transition between linear (elastic) and curved (plastic) part in Fig. 11a is lower for CuCr1-K1100 composite than for Cu-K1100 composite. This means that the matrix yield stress in the CuCr1-K1100 composite is reached sooner, what is consistent with the tendency to build up residual compressive stresses in CuCr1-K1100 composite and residual tensile stresses in Cu-K1100 composite as observed in the first cycle. This is also why the overall expansion in CuCr1-K1100 composite is lower.

The comparison of relative elongations of composites in T direction reveals permanent strains for both composites. The corresponding CTEs in Figs. 8 and 10 confirm that they are all above the CTE of matrix. This can be explained by the constant volume of the matrix during yielding [29]. As the temperature rises, the matrix is primarily stressed in compression along the fibre axis and it starts to yield at some point. Nevertheless, the matrix flow along the fibre axis is limited when the fibre/matrix bond is strong enough. At the same time, the matrix yielding transversely to the fibre axis is only little restricted enabling thus large transversal plastic strain [8]. The less perfect infiltration of Cu-K1100 composite with larger pores provides more space for the matrix to expand within the sample. This takes place during the first thermal cycle. Therefore, the permanent strain of this composite is smaller than that of CuCr1-K1100 where the stronger interfacial bonding is supposed.

The similarity of temperature dependences of relative elongations of both composites in the second and third cycles is obvious. One might expect that using CuCr1 and Cu matrices with different properties should yield more distinguished results. The similarity, however, can be further explained by the fact that nearly all Cr has been consumed by the fibre-matrix reaction and the matrix has become pure Cu. The main differences between both composites are actually chromium carbides found at the interface in CuCr1-K1100 composite.

The role of interface on the thermal expansion of Cu based composites reinforced with continuous unidirectionally aligned high modulus carbon fibres is not as apparent as in other composites. The main difference in L direction was the residual compression stress in the CuCr1-K1100 composite and residual tension in Cu-K1100 composite. Nevertheless, Cr content has led to better infiltration with fewer voids and pores. Pure Cu makes the infiltration difficult yielding definitely more voids. The proper infiltration with pure Cu is hardly feasible with larger samples. Anyway, the pores are not detrimental to the expansion of the com-

posites. They can absorb the expanding matrix what results in smaller relative elongations as in the case of more perfectly impregnated structures.

5. Conclusions

The influence of Cr on structure and thermal expansion of copper matrix composites reinforced with unidirectionally aligned continuous high modulus C fibres was studied in this work. The addition of 1 wt.% of Cr has dramatically improved the wetting of K1100 fibres with the matrix alloy CuCr1, facilitating thus the composite preparation via gas pressure infiltration. Due to the chemical reaction with K1100 fibres a reactive interfacial bonding has been formed.

The lack of wetting made the infiltration in the Cu-K1100 system quite a difficult task. It can hardly be controlled in an industrial scale. The composite structure exhibited larger voids and weak interfacial bonding.

The thermal expansions of both composites were different in the first cycle in *L* and *T* directions, due to different residual stresses appearing as a consequence of manufacturing process.

The thermal expansion in second and third cycles is distinguished by two knees at about 100 °C and 200 °C. The first knee is related to the start of the stress relief after the compression yield stress of the matrix had been reached. The second knee is to be associated with the decrease of the composite interfacial bonding strength.

The effect of Cr on the thermal expansion of copper based composites reinforced with densely packed unidirectionally aligned continuous high modulus C fibres was not found as apparent as in short fibre or particulate reinforced composites.

Acknowledgements

This work has been performed within the framework of the Integrated European Project ExtreMat (contract NMP-CT-2004-500253) and with financial support by the European Community. It only reflects the view of the authors and the EC is not liable for any use of the information contained therein. The financial support of Scientific Grant Agency under the contract VEGA 2/7173/27 is highly appreciated.

References

- [1] ZWEBEN, C.: Adv. Mater. Proc., 163, 2005, p. 33.
- [2] ZWEBEN, C.: Power Electron. Technol., 32, 2006, p. 40.
- [3] WEBER, L.—TAVANGAR, R.: Scripta Mater., 57, 2007, p. 988.
- [4] SCHUBERT, T.—CIUPINSKI, L.—ZIELIŃSKI, W.—MICHALSKI, A.—WEIßGÄRBER, T.—KIEBACK, B.: Scripta Mater., 58, 2008, p. 263.
- [5] SCHUBERT, T.—TRINDADE, B.—WEIßGÄRBER, T.—KIEBACK, B.: Mater. Sci. Eng. A, 475, 2008, p. 39.
- [6] LUO, X.—YANG, Y.—LIU, C.—XU, T.—YUAN, M.—HUANG, B.: Scripta Mater., 58, 2008, p. 401.
- [7] WANG, Y. L.—WAN, Y. Z.—CHENG, G. X.—DONG, X. H.—ZHOU, F. G.: Acta Mater. Compos. Sinica, 15, 1998, p. 83.
- [8] KÚDELA, S. Jr.—RUDAJEVOVÁ, A.—KÚDELA, S.: Mater. Sci. Eng. A, 462, 2007, p. 239.
- [9] LIN, M. H.—BUCHGRABER, W.—KORB, G.—KAO, P. W.: Scripta Mater., 46, 2002, p. 169.
- [10] KORAB, J.: Thermophysical properties of continuous carbon fibre reinforced copper matrix composites. [PhD Thesis]. Matrix Verlag 1999, ISBN 3-9501075-2-5.
- [11] SIMANČÍK, F.—ŠEBO, P.: Kovove Mater., 29, 1991, p. 358.
- [12] YOUNG, R. M. K.: Mat. Sci. Tech., 6, 1990, p. 548.
- [13] MORTENSEN, A.—CORNIE, J.: Met. Trans. A, 18A, 1987, p. 1160.
- [14] MORTIMER, D.—NICHOLAS, M.: J. Mater. Sci., 5, 1970, p. 149.
- [15] MORTIMER, D.—NICHOLAS, M.: J. Mater. Sci., 8, 1973, p. 640.
- [16] NOGI, K.—OSUGI, Y.—OGINO, K.: Iron Steel Inst. Jpn., 30, 1990, p. 64.
- [17] DEVINCENT, S. M.—MICHAL, G. M.: Met. Trans. A, 24A, 1993, p. 53.
- [18] VOITOVITCH, R.—MORTENSEN, A.—HODAJ, F.—EUSTATHOPOULOS, N.: Acta Mater., 47, 1999, p. 1117.
- [19] IŽDINSKÝ, K.—SIMANČÍK, F.—KORÁB, J.—KRAMER, I.—ŠTEFÁNIK, P.—KAVECKÝ, Š.—ŠRÁMKOVÁ, T.—CSUBA, A.—ZEMÁNKOVÁ, M.: Kovove Mater., 44, 2006, p. 327.
- [20] RUDAJEVOVÁ, A.—KÚDELA, S. Jr.—KÚDELA, S.—LUKÁČ, P.: Scripta Mater., 53, 2005, p. 1417.
- [21] RUDAJEVOVÁ, A.—LUKÁČ, P.: Acta Mater., 51, 2003, p. 5579.
- [22] KAMAL, S.—JAYAGANTHAN, R.—PRAKASH, S. et al.: J. Alloys and Compounds, 463, 2008, p. 358.
- [23] NAM, T. H.—REQUENA, G.—DEGISCHER, P.: Composites: Part A, 39, 2008, p. 856.
- [24] RUDAJEVOVÁ, A.—MUSIL, O.: Kovove Mater., 43, 2005, p. 210.
- [25] RUDAJEVOVÁ, A.—LUKÁČ, P.: Kovove Mater., 46, 2008, p. 145.
- [26] LUKÁČ, P.—RUDAJEVOVÁ, A.: Kovove Mater., 41, 2003, p. 281.
- [27] KUMAR, S.—INGOLE, S.—DIERINGA, H.—KAINER, K. U.: Comp. Sci. Tech., 63, 2003, p. 1805.
- [28] DUTTA, I.: Acta Mater., 48, 2000, p. 1055.
- [29] NASSINI, H. E.—MORENO, M.—GONZALES, O. C.: J. Mater. Sci., 36, 2001, p. 2759.